Progress In Electromagnetics Research Letters, Vol. 27, 101–115, 2011

APPLICATIONS OF A THREE-DIMENSIONAL FDTD METHOD WITH WEAKLY CONDITIONAL STABILITY TO THE ANALYSIS OF MICROSTRIP FILTERS WITH FINE SCALE STRUCTURES

J. Lan[1,*], Y. Yang[1,2], and J. Y. Dai[1]

[1]College of Electronics and Information Engineering, Nanjing University of Aeronautics and Astronautics, Nanjing 210016, China

[2]National Key Laboratory of Millimeter Wave, Southeast University, Nanjing 210096, China

Abstract—In three-dimensional space, the hybrid implicit-explicit finite-difference time-domain (HIE-FDTD) method is weakly conditionally stable, only determined by two space-discretizations, which is very useful for problems with fine structures in one direction. Its numerical dispersion errors with nonuniform cells are discussed and compared in this paper. To enlarge the applicable field of the HIE-FDTD method to open space, the absorbing boundary conditions (ABCs) for this method are also introduced and applied. Two microstrip filters with fine scale structures in one direction are solved by the HIE-FDTD method. Conventional FDTD method and alternating-direction implicit FDTD (ADI-FDTD) method are also used for comparing. Results analyzed by the HIE-FDTD method agree well with those from conventional FDTD, and the required central process unit (CPU) time is much less than that of the ADI-FDTD method.

1. INTRODUCTION

The finite-difference time-domain (FDTD) method [1] has been applied to varieties of electromagnetic analysis fields for its convenience and accuracy. Nevertheless, as an explicit time-stepping scheme, the FDTD method must be satisfied with the Courant-Friedrich-Levy (CFL) condition, which makes it unavailable for electrically fine scale structures.

Received 22 August 2011, Accepted 13 October 2011, Scheduled 5 November 2011

* Corresponding author: Jing Lan (vipjinga@sina.com).

To eliminate the CFL constraint on the time step size in conventional FDTD, some unconditionally stable implicit methods, such as ADI-FDTD method [2–4], Crank-Nicloson FDTD (CN-FDTD) method [5], are advanced. These implicit methods have been proved to be very computationally efficient when the time step exceeding the CFL condition, but they also have restrictions. It is well known that the ADI-FDTD method will result in numerical dispersion error for larger step size. The CN-FDTD method has less dispersion and higher accuracy, but it is very memory and CPU-time expensive, which makes it inefficient in fine scale problems.

Recently, a new method — HIE-FDTD method [6, 7] in 3-D case based on the advantage of ADI-FDTD method has been developed. Similarly but not identically, the HIE-FDTD method keeps a weaker CFL condition than conventional FDTD method, and the time step is only determined by two space discretizations in this scheme. It only needs a single sub-iteration (two tri-diagonal matrices and four explicit updates) while the ADI-FDTD method needs two (six tri-diagonal matrices and six explicit updates).

In this paper, the stability of HIE-FDTD method is derived. As the HIE-FDTD method is very useful for problems with fine structures in one direction, its numerical dispersion errors with nonuniform cells is discussed and compared. The HIE-FDTD method with Mur's ABC [8] is developed and operated to simulate two microstrip filters with fine scale structures in one direction. The numerical results from conventional FDTD method and ADI-FDTD method are also rendered for comparing. It is exhibited that the HIE-FDTD method has higher approximation with conventional FDTD method than the ADI-FDTD method especially for larger time step size, and the CPU time is much shorter than that of the ADI-FDTD method. It is very useful for problems that need a fine mesh in one direction.

2. FORMULATION FOR 3-D HIE-FDTD METHOD

In an isotropic lossless region with permittivity ε and permeability μ, assuming the narrow side along the z direction, the matrix formulations of the HIE-FDTD method for a full 3-D wave are presented in Equation (1). It is shown that the calculation for one discrete time

step is performed using only one procedure.

$$\begin{bmatrix} 1 & 0 & 0 & 0 & \frac{\Delta t}{\varepsilon}\frac{\partial}{2\partial z} & -\frac{\Delta t}{\varepsilon}\frac{\partial}{\partial y} \\ 0 & 1 & 0 & -\frac{\Delta t}{\varepsilon}\frac{\partial}{2\partial z} & 0 & \frac{\Delta t}{\varepsilon}\frac{\partial}{\partial x} \\ 0 & 0 & 1 & 0 & 0 & 0 \\ 0 & -\frac{\Delta t}{\mu}\frac{\partial}{2\partial z} & \frac{\Delta t}{\mu}\frac{\partial}{\partial y} & 1 & 0 & 0 \\ \frac{\Delta t}{\mu}\frac{\partial}{2\partial z} & 0 & -\frac{\Delta t}{\mu}\frac{\partial}{\partial x} & 0 & 1 & 0 \\ 0 & 0 & 0 & 0 & 0 & 1 \end{bmatrix} \begin{bmatrix} E_x^{n+1} \\ E_y^{n+1} \\ E_z^{n+\frac{1}{2}} \\ H_x^{n+1} \\ H_y^{n+1} \\ H_z^{n+\frac{1}{2}} \end{bmatrix}$$

$$= \begin{bmatrix} 1 & 0 & 0 & 0 & -\frac{\Delta t}{\varepsilon}\frac{\partial}{2\partial z} & 0 \\ 0 & 1 & 0 & \frac{\Delta t}{\varepsilon}\frac{\partial}{2\partial z} & 0 & 0 \\ 0 & 0 & 1 & -\frac{\Delta t}{\varepsilon}\frac{\partial}{\partial y} & \frac{\Delta t}{\varepsilon}\frac{\partial}{\partial x} & 0 \\ 0 & \frac{\Delta t}{\mu}\frac{\partial}{2\partial z} & 0 & 1 & 0 & 0 \\ -\frac{\Delta t}{\mu}\frac{\partial}{2\partial z} & 0 & 0 & 0 & 1 & 0 \\ \frac{\Delta t}{\mu}\frac{\partial}{\partial y} & -\frac{\Delta t}{\mu}\frac{\partial}{\partial x} & 0 & 0 & 0 & 1 \end{bmatrix} \begin{bmatrix} E_x^n \\ E_y^n \\ E_z^{n-\frac{1}{2}} \\ H_x^n \\ H_y^n \\ H_z^{n-\frac{1}{2}} \end{bmatrix} \quad (1)$$

Firstly, from this matrix, $E_z^{n+\frac{1}{2}}$ and $H_z^{n+\frac{1}{2}}$ components can be calculated explicitly. Substituting $H_z^{n+\frac{1}{2}}$ components and equations for H_y^{n+1} into equations for E_x^{n+1}, then E_x components are derived as Equation (2):

$$\begin{aligned} &\left[1+\frac{\Delta t^2}{2\varepsilon\mu\Delta z^2}\right] E_x^{n+1}\left(i+\frac{1}{2},j,k\right) \\ &-\frac{\Delta t^2}{4\varepsilon\mu\Delta z^2}\left[E_x^{n+1}\left(i+\frac{1}{2},j,k+1\right)+E_x^{n+1}\left(i+\frac{1}{2},j,k-1\right)\right] \\ =\ &\left[1-\frac{\Delta t^2}{2\varepsilon\mu\Delta z^2}\right] E_x^{n}\left(i+\frac{1}{2},j,k\right) \\ &-\frac{\Delta t}{\varepsilon}\frac{1}{\Delta z}\left[H_y^{n}\left(i+\frac{1}{2},j,k+\frac{1}{2}\right)-H_y^{n}\left(i+\frac{1}{2},j,k-\frac{1}{2}\right)\right] \\ &+\frac{\Delta t}{\varepsilon}\frac{1}{\Delta y}\left[H_z^{n+\frac{1}{2}}\left(i+\frac{1}{2},j+\frac{1}{2},k\right)-H_z^{n+\frac{1}{2}}\left(i+\frac{1}{2},j-\frac{1}{2},k\right)\right] \\ &+\frac{\Delta t^2}{4\varepsilon\mu\Delta z^2}\left[E_x^{n}\left(i+\frac{1}{2},j,k+1\right)+E_x^{n}\left(i+\frac{1}{2},j,k-1\right)\right] \\ &-\frac{\Delta t^2}{2\varepsilon\mu\Delta x\Delta z}\left[E_z^{n+\frac{1}{2}}\left(i+1,j,k+\frac{1}{2}\right)-E_z^{n+\frac{1}{2}}\left(i,j,k+\frac{1}{2}\right)\right. \\ &\left.-E_z^{n+\frac{1}{2}}\left(i+1,j,k-\frac{1}{2}\right)+E_z^{n+\frac{1}{2}}\left(i,j,k-\frac{1}{2}\right)\right] \end{aligned} \quad (2)$$

Similarly, E_y components are obtained by a similar equation. E_x

and E_y components are updated implicitly after solving the above tri-diagonal matrix equations. Then H_x and H_y components can be calculated explicitly. Therefore, at each time step, two tri-diagonal matrices and four explicit updates should be solved in this HIE-FDTD method. Comparatively, the ADI-FDTD method needs to solve six tri-diagonal matrices and six explicit updates for a full update, which makes it computationally inefficient.

3. NUMERICAL STABILITY AND NUMERICAL DISPERSION ANALYSIS FOR 3-D HIE-FDTD METHOD

3.1. Numerical Stability for 3-D HIE-FDTD Method

In the matrix of Equation (1), we let:

$$\frac{\partial}{\partial u} f = j_0 \frac{1}{\Delta u/2} \sin\left(\frac{k_u \Delta u}{2}\right) f = 2 j_0 W_u f \tag{3}$$

and

$$V_u^n(i,j,k) = V_{0u} \zeta^n f(i,j,k) \tag{4}$$

where $f(i,j,k) = e^{j_0(ik_x\Delta x + jk_y\Delta y + kk_z\Delta z)}$, $j_0 = \sqrt{-1}$, $W_u = \frac{1}{\Delta u}\sin(\frac{k_u\Delta u}{2})$, k_u are wave numbers, $u = x,\ y,\ z$, $V = E,\ H$, and ζ indicates the growth factor.

The new matrix is represented as:

$$\begin{bmatrix} \zeta-1 & 0 & 0 & 0 & p\,(\zeta{+}1)\,j_0 W_z & -2p\zeta j_0 W_y \\ 0 & \zeta-1 & 0 & -p\,(\zeta{+}1)\,j_0 W_z & 0 & 2p\zeta j_0 W_x \\ 0 & 0 & \zeta-1 & 2pj_0 W_y & -2pj_0 W_x & 0 \\ 0 & -q\,(\zeta{+}1)\,j_0 W_z & 2q\zeta j_0 W_y & \zeta-1 & 0 & 0 \\ q\,(\zeta{+}1)\,j_0 W_z & 0 & -2q\zeta j_0 W_x & 0 & \zeta-1 & 0 \\ -2qj_0 W_y & 2qj_0 W_x & 0 & 0 & 0 & \zeta-1 \end{bmatrix} \begin{bmatrix} E_{0x}\zeta^n f \\ E_{0y}\zeta^n f \\ E_{0z}\zeta^{n-\frac{1}{2}} f \\ H_{0x}\zeta^n f \\ H_{0y}\zeta^n f \\ H_{0z}\zeta^{n-\frac{1}{2}} f \end{bmatrix} = 0 \tag{5}$$

where $p = \frac{\Delta t}{\varepsilon},\ q = \frac{\Delta t}{\mu},\ u = x,\ y,\ z$.

In order for this matrix to have a nonzero solution, the determinant of its coefficient should be zero. Then we can obtain a polynomial about the growth factor ζ:

$$(\zeta-1)^2 \left[(1+r_z)\zeta^2 - 2\,(1-2r_x-2r_y-r_z)\,\zeta + 1 + r_z\right]^2 = 0 \tag{6}$$

where $r_u = (c\Delta t)^2 W_u^2,\ u = x,\ y,\ z$.

Then $\zeta_1 = \zeta_2 = 1$, $\zeta_3 = \zeta_4 = \zeta_5 = \zeta_6 = \frac{(1-2r_x-2r_y-r_z)\pm 2\sqrt{-(1-r_x-r_y)(r_x+r_y+r_z)}}{1+r_z}$

To satisfy the $|\zeta_i| \leq 1$ condition:

$$r_x + r_y \leq 1 \tag{7}$$

Derived from the above formulations, we can obtain the stability condition of the HIE-FDTD method is solved as following:

$$\Delta t_{HIE\text{-}FDTD} \leq \frac{1}{c} \frac{1}{\sqrt{\frac{1}{(\Delta x)^2} + \frac{1}{(\Delta y)^2}}} \tag{8}$$

In conventional 3-D FDTD method, the stability condition is the CFL condition [1] expressed as:

$$\Delta t_{FDTD} \leq \frac{1}{c} \frac{1}{\sqrt{\frac{1}{(\Delta x)^2} + \frac{1}{(\Delta y)^2} + \frac{1}{(\Delta z)^2}}} \tag{9}$$

Equation (8) shows that the HIE-FDTD method is only determined by two spatial discretions in three dimensional space. If the computational problem has fine scale structures in z-direction, the maximum time step of conventional FDTD method will be very small, which makes conventional FDTD computationally inefficient, but the HIE-FDTD method is not limited by the fine scale structures. As a result, the CPU time for the HIE-FDTD method can be saved compared with that of conventional FDTD method.

3.2. Numerical Dispersion Analysis for 3-D HIE-FDTD Method

In this paper, the HIE-FDTD method is employed to solve the problems with fine scale structures in one direction, so the dispersion errors of the HIE-FDTD method [9] with nonuniform cells is discussed. Conventional FDTD method and ADI-FDTD method are compared. The CFLN [1] (Courant-Friedrich-Levy Number) of both the HIE-FDTD method and conventional FDTD method are the largest values which satisfy their own CFL conditions. The ADI-FDTD method has the same CFLN as the HIE-FDTD method for comparison. In Figs. 1(a)–(e), the normalized numerical phase speeds of the three methods are shown respectively with $\Delta x = \Delta y = 5\Delta z = \lambda/10$, and θ set as 0°, 22.5°, 45°, 67.5°, 90°.

As shown in Fig. 1(a), when $\theta = 0°$ ($k_x = k\sin\theta\cos\phi = 0$, $k_y = k\sin\theta\sin\phi = 0$, $k_z = k\cos\theta = k$), along the z axis, the numerical dispersion error of the HIE-FDTD method is as large as that of the ADI-FDTD method. In Figs. 1(b)–(e), as θ increases, the

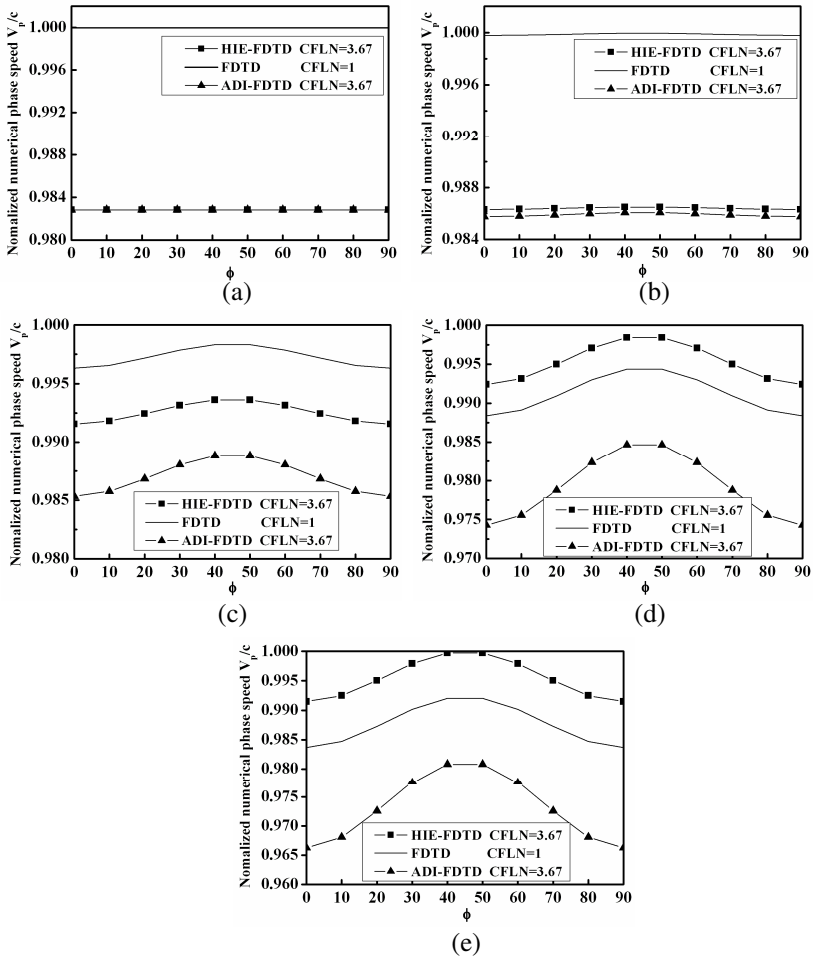

Figure 1. Comparison of the normalized numerical phase speed for different methods with $\theta = 0°$, $22.5°$, $45°$, $67.5°$, $90°$ when $\Delta x = \Delta y = 5\Delta z = \lambda/10$.

dispersion error of the HIE-FDTD method ameliorates and approaches conventional FDTD method, while the ADI-FDTD method [10] deteriorates unfortunately.

In summarizing the above results, it can be concluded that the numerical dispersion of the HIE-FDTD method is better than that of the ADI-FDTD method, although the numerical dispersions of the two methods are both the same along the z axis direction for the z axis is not the diagonal direction when updating E_u ($u = x,\ y,\ z$) components.

4. IMPLEMENTION OF MUR'S ABC IN THE 3-D HIE-FDTD METHOD

To enlarge the applicable field of the HIE-FDTD method to open space and semi-open space problems, ABCs for the HIE-FDTD method are presented in this paper. The Mur's ABC [8, 15] is chosen to develop in the HIE-FDTD method for its high efficiency while the commonly-used PML ABC [11–14] is time-consuming in 3-D space, which is the limitation of the PML ABC. Analyzing with Mur's ABCs, space will be divided into three sections (see Fig. 2), and the inner is the free space, six borders

As an explicit direction in the updating step, the E_z ($i = 1 \sim i_{\max} - 1$) variable at the borders boundary region $y = 0$ and $y = j_{\max}$ of the Mur's ABCs is (v is the speed of light in the medium):

$$\begin{aligned} E_z^{n+1}\left(i,0,k+\frac{1}{2}\right) &= -\frac{v\Delta t-\Delta y}{v\Delta t+\Delta y}\left(E_z^{n+1}\left(i,1,k+\frac{1}{2}\right)-E_z^n\left(i,0,k+\frac{1}{2}\right)\right) \\ &\quad + E_z^n\left(i,1,k+\frac{1}{2}\right) \quad \left(k=\frac{1}{2},\ k=k_{\max}-\frac{1}{2}\right) \\ E_z^{n+1}\left(i,j_{\max},k+\frac{1}{2}\right) &= -\frac{v\Delta t-\Delta y}{v\Delta t+\Delta y}\left(E_z^{n+1}\left(i,j_{\max}-1,k+\frac{1}{2}\right)\right. \\ &\quad \left. -E_z^n\left(i,j_{\max},k+\frac{1}{2}\right)\right)+E_z^n\left(i,j_{\max}-1,k+\frac{1}{2}\right) \end{aligned} \tag{10}$$

And the E_z variable at the corners $y = 0$ and $y = j_{\max}$ of the Mur's ABCs is:

$$\left[\frac{1}{c}\frac{\partial^2}{\partial x\partial t}-\frac{1}{c^2}\frac{\partial^2}{\partial t^2}+\frac{1}{2}\left(\frac{\partial^2}{\partial y^2}+\frac{\partial^2}{\partial z^2}\right)\right]E_z\left(i,y,k+\frac{1}{2}\right)=0 \quad \left(k=1\frac{1}{2}\sim k_{\max}-1\frac{1}{2}\right) \tag{11}$$

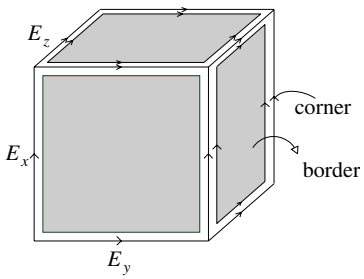

Figure 2. The schematic of Mur's ABC.

As implicit directions in the updating step, the implementation of the Mur's first order ABC for E_x and E_y should be applied inside the tri-diagonal matrix. Taking the E_x variable for example, it can be updated by the tri-diagonal matrix when E_x ($i = \frac{1}{2} \sim i_{\max} - \frac{1}{2};\ j = 1 \sim j_{\max} - 1;\ k = 0 \sim k_{\max}$):

$$AX = Y \qquad A = \begin{bmatrix} b_0 & c_0 & 0 & \cdots & 0 \\ a_1 & b_1 & c_1 & \cdots & 0 \\ 0 & \cdots & \ddots & \cdots & \vdots \\ & \vdots & & & \\ 0 & \cdots & & a_{k_{\max}} & b_{k_{\max}} \end{bmatrix},$$

$$X = \begin{bmatrix} E_x^{n+1}\left(i+\frac{1}{2}, j, 0\right) \\ \vdots \\ E_x^{n+1}\left(i+\frac{1}{2}, j, k\right) \\ \vdots \\ E_x^{n+1}\left(i+\frac{1}{2}, j, k_{\max}\right) \end{bmatrix}, \quad Y = \begin{bmatrix} d_0 \\ \vdots \\ \vdots \\ d_k \\ \vdots \\ \vdots \\ d_{k_{\max}} \end{bmatrix} \tag{12}$$

While at the corners $z = 0$ and $z = k_{\max}$, the coefficients of the matrix needed special consideration and ABC should be used. The field component E_x ($i = \frac{1}{2} \sim i_{\max} - \frac{1}{2};\ j = 1 \sim j_{\max} - 1;\ k = 0,\ k = k_{\max}$) at the boundary $z = 0$ and $z = k_{\max}$ becomes Equation (13) and Equation (14), when E_x ($i = \frac{1}{2} \sim i_{\max} - \frac{1}{2};\ j = 0,\ j = j_{\max};\ k = 0,\ k = k_{\max}$) at the boundary $j = 0$ and $j = j_{\max}$ is not concluded in the tri-diagonal matrix. E_x can be solved by the Mur's first order ABC directly.

$$\begin{aligned} & E_x^{n+1}\left(i+\frac{1}{2}, j, 0\right) - \frac{v\Delta t - \Delta z}{v\Delta t + \Delta z} E_x^{n+1}\left(i+\frac{1}{2}, j, 1\right) \\ =& E_x^{n}\left(i+\frac{1}{2}, j, 1\right) - \frac{v\Delta t - \Delta z}{v\Delta t + \Delta z} E_x^{n}\left(i+\frac{1}{2}, j, 0\right) \\ & b_0 = 1, \quad c_0 = -\frac{v\Delta t - \Delta z}{v\Delta t + \Delta z}, \\ & d_0 = E_x^{n}\left(i+\frac{1}{2}, j, 1\right) - \frac{v\Delta t - \Delta z}{v\Delta t + \Delta z} E_x^{n+1}\left(i+\frac{1}{2}, j, 0\right) \end{aligned} \tag{13}$$

$$\begin{aligned}
&E_x^{n+1}\left(i+\frac{1}{2},j,k_{\max}\right)-\frac{v\Delta t-\Delta z}{v\Delta t+\Delta z}E_x^{n+1}\left(i+\frac{1}{2},j,k_{\max}-1\right)\\
=&E_x^{n}\left(i+\frac{1}{2},j,k_{\max}-1\right)-\frac{v\Delta t-\Delta z}{v\Delta t+\Delta z}E_x^{n}\left(i+\frac{1}{2},j,k_{\max}\right)\\
&a_{k_{\max}}=-\frac{v\Delta t-\Delta z}{v\Delta t+\Delta z},\quad b_{k_{\max}}=1,\\
&d_{k_{\max}}=E_x^{n}\left(i+\frac{1}{2},j,k_{\max}\right)-\frac{v\Delta t-\Delta z}{v\Delta t+\Delta z}E_x^{n+1}\left(i+\frac{1}{2},j,k_{\max}\right)
\end{aligned}\tag{14}$$

The ABCs of the E_y variable is similar to the ABCs of the above E_x.

It is known that the Mur's ABC implemented in the ADI-FDTD method must be the Mur's first order ABC [14]. However, the Mur's second order ABC is implemented in the HIE-FDTD method in above formulations, which shows higher accuracy than the ADI-FDTD method.

5. NUMERICAL RESULTS AND COMPARISON

In order to give proof to the validity and effectiveness of the HIE-FDTD method in solving problems with fine structures in one direction, two novel planar microstrip filters are simulated by this method. Conventional FDTD method and ADI-FDTD method are also simulated for comparison.

5.1. Simulation for a Compact and Wideband Planar Microstrip Bandstop Filter

The planar microstrip bandstop filter (see Fig. 3) [16] is located on a substrate with $\varepsilon_r = 2.33$ and $h = 0.783\,\text{mm}$, and it is a bilaterally symmetry geometry. The input/output impedance of the feedline is $50\,\Omega$. We chose the FDTD cell size: $\Delta x = 0.783\,\text{mm}$, $\Delta y = 1.044\,\text{mm}$, $\Delta z = 0.2485\,\text{mm}$. Then the total number of the FDTD cells is $16 \times 42 \times 196$. This bandstop filter is excited by a 60 ps Gaussian pulse at one end of the structure (x-y plane, $z = 16\Delta z$), while the observation points 1 and 2 are located at the edges of the structure (x-y plane, $z_1 = 32\Delta z$ and $z_2 = 170\Delta z$). The boundaries are terminated with Mur's ABC.

Figure 4 shows the time domain voltage waveforms at observation 1 and observation 2, respectively. Simulation results show that with a larger time step than that of conventional FDTD method, the HIE-FDTD method is in good agreement with conventional FDTD method, while the ADI-FDTD method exhibits an obvious splitting error.

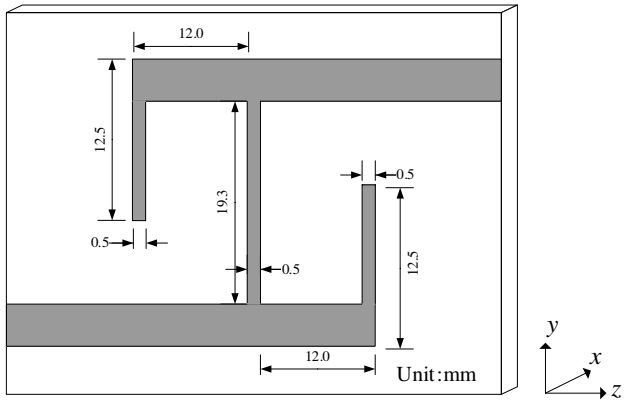

Figure 3. The geometry of the microstrip planar bandstop filter.

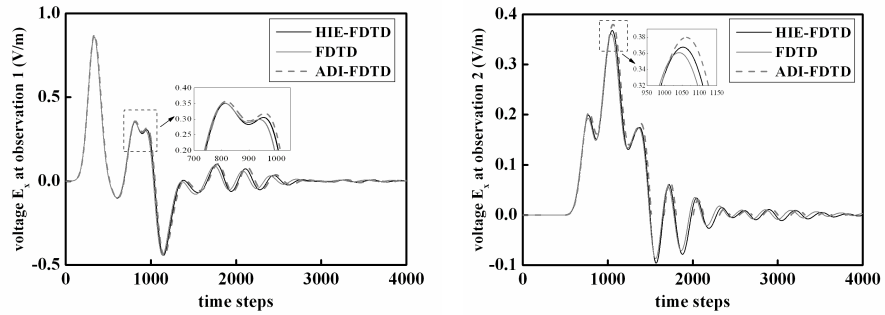

Figure 4. The results of time domain waveforms for voltages at observation 1 and observation 2 calculated by the HIE-FDTD method ($\Delta t = 2.0894\,\text{ps}$), conventional FDTD method ($\Delta t = 0.7705\,\text{ps}$) and the ADI-FDTD method ($\Delta t = 2.0894\,\text{ps}$).

In Fig. 5, the 2-port S parameters are calculated on the base of above time domain data by the three methods. Compared with the result of conventional FDTD method, the error of the HIE-FDTD method is in the allowable range.

The simulation time for the bandstop filter by the HIE-FDTD method, conventional FDTD method and ADI-FDTD method are summarized in Table 1. From Table 1, we can see that with the weakly conditionally stability, the HIE-FDTD method has a larger Δt than conventional FDTD method. The CPU time for the HIE-FDTD method can be shorter than conventional FDTD method. And the CPU time for the HIE-FDTD method is almost 1/2 of that for the

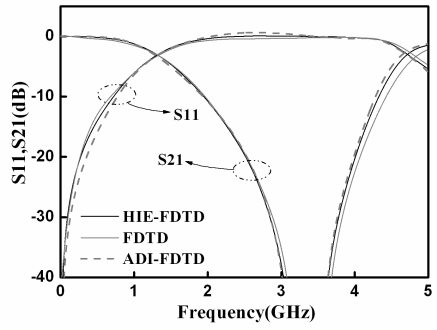

Figure 5. The 2-port S parameters for the bandstop filter calculated by the HIE-FDTD method, conventional FDTD method and the ADI-FDTD method.

Table 1. CPU times for the bandstop filter in the simulation by the HIE-FDTD method, conventional FDTD method and the ADI-FDTD method.

	HIE-FDTD ($\Delta t = 2.0894$ ps)	FDTD ($\Delta t = 0.7705$ ps)	ADI-FDTD ($\Delta t = 2.0894$ ps)
CPU times	268.73 s	356.31 s	497.92 s

ADI-FDTD method, so the HIE-FDTD method has higher efficiency than the ADI-FDTD method.

5.2. Simulation for a Microstrip Dual-band Bandpass Filter

The microstrip dual-band bandpass filter (see Fig. 6) [17] is located on a substrate with $\varepsilon_r = 9.8$ and $h_1 = 1.27$ mm. The FDTD cell size is chosen to be $\Delta x = 0.63$ mm, $\Delta y = 0.55$ mm, $\Delta z = 0.05$ mm. The total number of the FDTD cells is $8 \times 46 \times 650$. The bandpass filter is excited by a 100 ps modulated-Gaussian pulse at the point (x-y plane, $z = 24\Delta z$), while the observation points 1 and 2 are located at the two ends of this structure (x-y plane, $z_1 = 48\Delta z$ and $z_2 = 620\Delta z$). The Mur's ABC is used for the termination.

Figure 7 shows the time domain voltage waveforms at observation 1 and observation 2, respectively. It is shown that with a larger time step than conventional FDTD method, both the HIE-FDTD method and ADI-FDTD method have an obvious dispersion error, but the dispersion error of the HIE-FDTD method is smaller than that of the ADI-FDTD method.

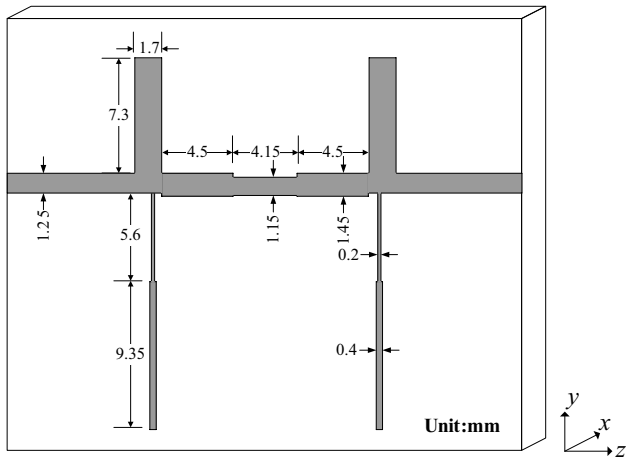

Figure 6. Configuration of the microstrip dual-band bandpass filter.

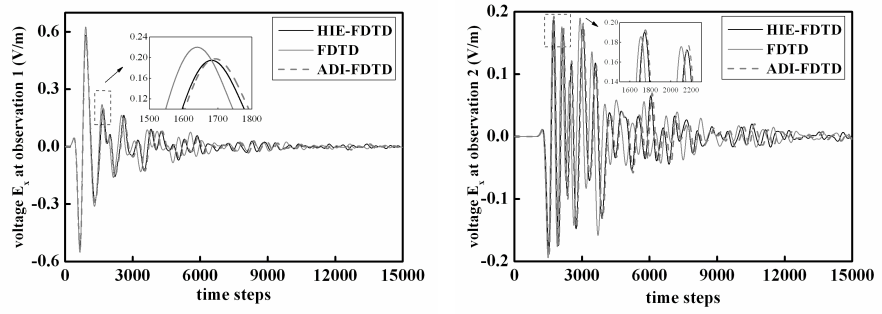

Figure 7. The results of time domain waveforms for voltages at observation 1 and at observation 2 calculated by the HIE-FDTD method ($\Delta t = 1.3820$ ps), conventional FDTD method ($\Delta t = 0.1656$ ps) and the ADI-FDTD method ($\Delta t = 1.3820$ ps).

In Fig. 8, the 2-port S parameters are calculated by the three methods. Compared with the result of conventional FDTD method, the error of the HIE-FDTD method is in the allowable range.

The simulation time for the dual-band bandpass filter by the HIE-FDTD method, conventional FDTD method and ADI-FDTD method are summarized in Table 2. From Table 2, we can again validate that the CPU time for the HIE-FDTD method is almost 1/2 of that for the ADI-FDTD method, and the computation time can be shorter than conventional FDTD method for using a larger time step.

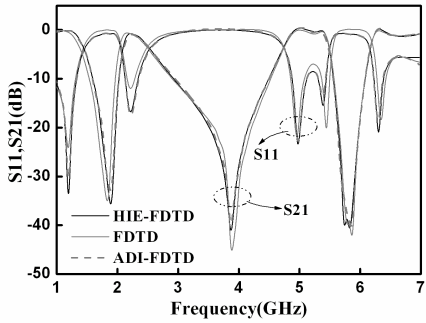

Figure 8. The 2-port S parameters for the dual-band bandpass filter calculated by the HIE-FDTD method, conventional FDTD method and the ADI-FDTD method.

Table 2. CPU times for the dual-band bandpass filter in the simulation by the HIE-FDTD method, conventional FDTD method and the ADI-FDTD method.

	HIE-FDTD ($\Delta t = 1.3820$ ps)	FDTD ($\Delta t = 0.1656$ ps)	ADI-FDTD ($\Delta t = 1.3820$ ps)
CPU times	629.03 s	2407.92 s	1397.61 s

From the above comparison in time domain and frequency domain parameters for two microstrip filters with fine scale structures in one direction, the HIE-FDTD method is more efficient than conventional FDTD and higher accuracy than the ADI-FDTD method.

6. CONCLUSION

In this paper, the 3-D weakly conditionally stability HIE-FDTD method with Mur's ABC is developed and implemented to analyze two microstrip filters with fine structures in one direction. Its stability is derived, only determined by Δx and Δy, and its numerical dispersion errors with nonuniform cells is discussed and compared. Compared with conventional FDTD method and ADI-FDTD method, it is exhibited that the HIE-FDTD method has a higher efficiency than conventional FDTD method and less deviation than the ADI-FDTD method. The CPU time for the HIE-FDTD method can be reduced to nearly 1/2 that of the ADI-FDTD method. The HIE-FDTD method with Mur's ABC is especially applicable to structures with very fine size in one direction, which is confirmed by numerical examples.

ACKNOWLEDGMENT

The authors acknowledge the funding from National Natural Science Foundation of China under Contract Numbers 60901007 and 61172024 and from Open Research Program in National Key Laboratory of Millimeter Waves under Contract Number K200906.

REFERENCES

1. Taflove, A., *Computational Electrodynamics: The Finite-difference Time-domain Method*, Artech House, Norwood, MA, 1996.
2. Namiki, T., "A new FDTD algorithm based on alternating direction implicit method," *IEEE Trans. Microwave Theory Tech.,* Vol. 47, 2003–2007, 1999.
3. Garcia, S. G., T. W. Lee, and S. C. Hagness, "On the accuracy of the ADI-FDTD method," *IEEE Antennas Wireless Propagat. Lett.,* Vol. 1, 31–34, 2002.
4. Heh, D. Y. and E. L. Tan, "Unified efficient fundamental ADI-FDTD schemes for lossy media," *Progress In Electromagnetics Research B*, Vol. 32, 217–242, 2011.
5. Yang, Y., Z. H. Fan, D. Z. Ding, and S. B. Liu, "Extend two-step preconditioning technique for the Crank-Nicolson finite-difference time-domain method to analyze the 3D microwave circuits," *International Journal of RF and Microwave Computer-aided Engineering*, Vol. 19, No. 4, 460–46, Jul. 2009.
6. Chen, J. and J. Wang, "Comparison between HIE-FDTD method and ADI-FDTD method," *Microwave Opt. Technol. Lett.*, Vol. 49, 1001–1005, May 2007.
7. Chen, J., J. Wang, and C. Tian, "Three-dimensional hybrid implicit explicit finite-difference time-domain method in the cylindrical coordinate system," *IEEE Trans. Antennas Propagat.,* Vol. 3, 1254–1261, Jan. 2009.
8. Mur, G., "Absorbing boundary conditions for the finite-difference approximation of the time-domain electromagnetic field equations," *IEEE Trans. Electromagn. Compat.*, Vol. 23, No. 4, 377–382, Nov. 1981.
9. Xiao, F., X. H. Tang, and L. Wang, "Stability and numerical dispersion analysis of a 3D hybrid implicit-explicit FDTD method," *IEEE Trans. Antennas Propagat.*, Vol. 56, 3346–3350, 2008.

10. Fu, W. M. and E. L. Tan, "Stability and dispersion analysis for ADI-FDTD method in lossy media," *IEEE Trans. Antennas Propagat.*, Vol. 55, No. 4, 1095–1102, Apr. 2007.
11. Gedney, S. D., "An anisotropic perfectly matched layer absorbing medium for the truncation of FDTD lattices," *IEEE Trans. Antennas and Propagat.*, Vol. 44, 1630–1639, 1996.
12. Yuan, W. and E. P. Li, "Numerical dispersion and impedance analysis for 3D perfectly matched layers used for truncation of the FDTD computations," *Progress In Electromagnetics Research*, Vol. 47, 193–212, 2004.
13. Shreim, A. M. and M. F. Hadi, "Integral PML absorbing boundary conditions for the high-order M24 FDTD algorithm," *Progress In Electromagnetics Research*, Vol. 76, 141–152, 2007.
14. Zhang, Y. Q. and D. B. Ge, "A unified FDTD approach for electromagnetic analysis of dispersive objects," *Progress In Electromagnetics Research*, Vol. 96, 155–172, 2009.
15. Tay, W. C. and E. L. Tan, "Implementation of the Mur first order absorbing boundary condition in efficient ADI-FDTD method," *IEEE Int. Symp. Antennas Propagat. USNC/URSI Nat. Radio Sci. Meeting,* Charleston, SC, Jun. 2009.
16. Cakir, G., "Design of a compact and wideband microstrip bandstop filter," *Microwave Opt. Technol. Lett.*, Vol. 50, 2612–2614, 2008.
17. Guan, X. H., S. Jiang, L. Shen, H. W. Liu, G. H. Li, and D. M. Xu, "A microstrip dual-band bandpass filter based on a novel admittance inverter," *IEEE MTT-S International Microwave Symposium*, 577–580, 2010.